

METADATA OF THE CLIMATE CHANGE KNOWLEDGE PORTAL



CLIMATE

HISTORICAL CLIMATE

CREDITS: Jones, P. D., and I. Harris, 2013: CRU TS3.21: **Climatic Research Unit (CRU) Time Series (TS)** Version 3.21 of High Resolution Gridded Data of Month-by-month Variation of Climate (Jan. 1901-Dec. 2012). 3.21 ed., U. o. E. Anglia, Ed., NCAS British Atmospheric Data Centre.

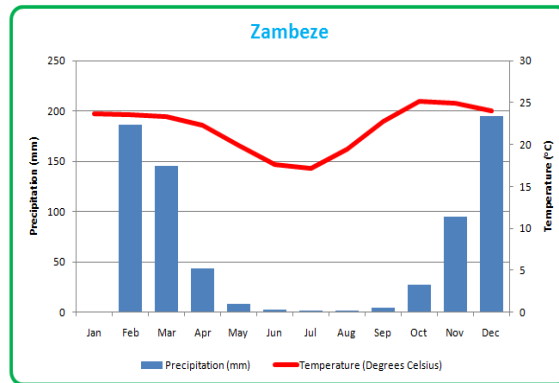
DESCRIPTION: Historical data are derived from 3 sources, all quality controlled by leading institutions in the field. To view the historical data, click on the map and under the 'Climate' tab click on the 'Historical' sub-tab. These are organized below under their potential use as follows:

- 1) Historical data to understand the seasonal CYCLE
- 2) Historical data to explore variability at the station level -
- 3) Historical data to evaluate how well Climate Models capture the regional seasonal cycle

1) Historical data to understand the seasonal CYCLE - click on the Historical data sub-tab

This gridded historical dataset is derived from observational data, and provides quality controlled temperature and rainfall values from thousands of weather stations worldwide, as well as derivative products including monthly climatologies and long term historical climatologies. The dataset is produced by the Climatic Research Unit (CRU) of University of East Anglia (UEA), and reformatted by International Water Management Institute (IWMI). CRU- (Gridded Product).

CRU data can be mapped to show the baseline climate and seasonality by month, for specific years, and for rainfall and temperature.

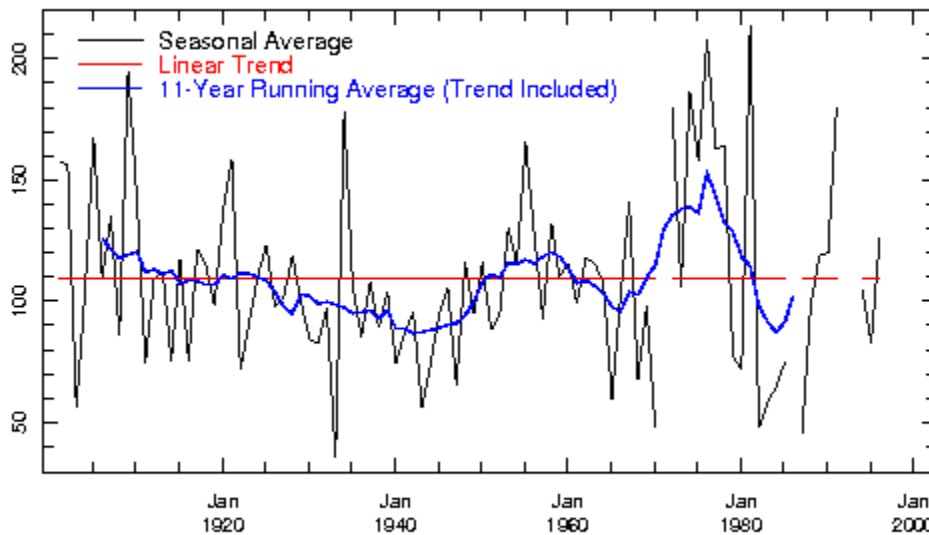


2) Historical data to explore variability at the station level - click on the Historical Variability Analysis Tool sub-tab.

Global Historical Climatology Network (GHCN) - provides station level, quality controlled, observational datasets for temperature and rainfall values from thousands of weather stations worldwide (GHCN), as well as derivative products including monthly climatologies and long term historical climatologies. To view the historical data, click on the map and under the 'Climate' tab click on the 'Historical' sub-tab- and Select the Historical Variability Analysis Button.

The Historical Variability Analysis Tool allows a user to investigate the historical variability of precipitation and temperature at various time scales (interannual, decadal, and long-term linear trend) over the 20th century near a user-selected location. An example output from this tool is presented below:

a. Jan-Mar Seasonal Average Station Precipitation Values, Decadal Variability, & Linear Trend

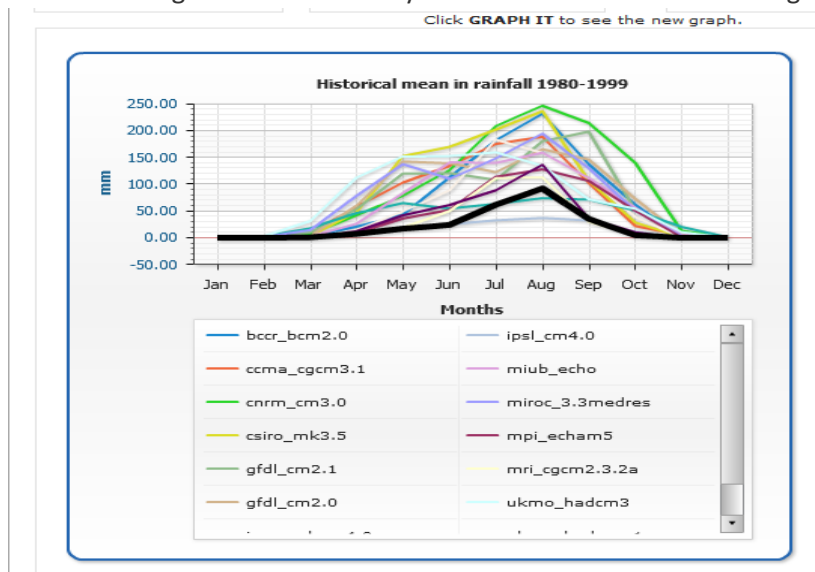


Station at (27.73E, 29.15S) TEYATEYANENG LESOTHO; Trend: -0.177106 mm/month per
[Seasonal average data in this graph](#) | [GIF image of this graph](#)

The historical period for these models is 1980-1999. CREDITS: IRI Columbia, [View Full Credits](#)

4) Historical data to evaluate how well Climate Models capture the regional seasonal cycle

Historical data to evaluate how well Climate Models capture the regional seasonal cycle - click on the 'Projection' sub-tab and click "more". Under the "Projections" sub-tab you can view the variations between different GCM's and National Centers for Environmental Prediction (NCEP) re-analysis data. NCEP offers a way to evaluate how well models capture the historical seasonal cycle of temperature and rainfall, and was developed by the [National Center for Atmospheric Research](#) by combining satellite and weather station information. In the portal, it has been modified to provide user-friendly information on rainfall and temperature and regridded to a common 2° grid matching the Global Climate Models. To view the historical data, click on the map and under the 'Climate' tab click on the 'FUTURE' sub-tab- - these data appear on the chart on the right hand side once you chart a model- as in the image below:



MAPS OF HISTORICAL CLIMATE

- "min temp of coldest month (Bioclim)"
- "max tem of warmest month (Bioclim)"
- "max temp of coldest month (Bioclim)"
- Rainfall
- Mean annual rainfall (Bioclim)
-

CREDITS: Hijmans, R.J., S.E. Cameron, J.L. Parra, P.G. Jones and A. Jarvis, 2005. Very high resolution interpolated climate surfaces for global land areas. [International Journal of Climatology 25: 1965-1978.](#)

LINK: <http://www.worldclim.org/bioclim>

How to access historical climate data in the CCKP: navigate through map>climate tab>historical tab

FUTURE CLIMATE

CMIP5 Dataset

CREDITS: National Center for Atmospheric Research (NCAR), Research Applications Laboratory

LINK: <http://www.ncar.org>

DESCRIPTION: The data used in this collection come from the CMIP5 distribution (Taylor et al. 2012). CMIP5 is the fifth iteration of a globally coordinated experiment collection using a previously agreed-upon suite of Representative Concentration Pathways – RCPs (Moss et al. 2010), which reflect different possible futures of distinct emissions, landuse change, and associated atmospheric radiative forcing. Up to CMIP3, these scenarios were called emission scenarios as presented in the Special Report on Emission Scenarios – SRES (Nakicenovic and Swart 2000), e.g., SRES scenarios A2, A1FI, A1B, B1. The scenarios considered here are the RCP-2.6, RCP-4.5, RCP-6.0 and RCP-8.5. The numbers attached to the RCPs represent the global mean radiative forcing in watts per square-meter achieved on a global average in each of the scenarios by the year 2100. More than 50 distinct models participated in the intercomparison activity, and many performed multiple simulations for selected scenarios to form ensembles. But only a subset of models completed all of the different scenarios with at least one simulation.

The CCKP-collection consists of 16 models (Table 1) that submitted monthly data for all of the RCPs and for which the data were readily available over the Earth System Grid. Four more models were identified that completed all experiments, but a few data gaps or quality issues prevented them from being included. These criteria ensure a consistent number and combination of models in each data product.

Model-Name	Modeling Center	Main Reference
bcc-csm1-1	Beijing Climate Center, China	Wu et al. (2013)
bcc-csm1-1-m	Beijing Climate Center, China	Wu et al. (2013)
CCSM4	National Center for Atmospheric Research, USA	Gent et al. (2011)
CESM1-CAM5	NSF-DOE-NCAR, USA	Hurrell and Co-Authors (2013)
CSIRO-Mk3-6-0	Commonwealth Scientific and Industrial Research Organization, Australia	Rotstayn et al. (2012)
FIO-ESM	The First Institute of Oceanography, China	Qiao et al. (2013)
GFDL-CM3	Geophysical Fluid Dynamics Laboratory, USA	Donner et al. (2011)
GFDL-ESM2M	Geophysical Fluid Dynamics Laboratory, USA	Dunne et al. (2012)
GISS-E2-H	Goddard Institute for Space Studies, USA	Schmidt et al. (2014)
GISS-E2-R	Goddard Institute for Space Studies, USA	Schmidt et al. (2014)
IPSL-CM5A-MR	Institut Pierre-Simon Laplace, France	Dufresne and Co-Authors (2013)
MIROC5	Atmosphere and Ocean Research Institute, National Institute for Environmental Studies, Japan Agency for Marine-Earth Science and Technology, Japan	Watanabe and Co-Authors (2010)
MIROC-ESM-CHEM	Japan Agency for Marine-Earth Science and Technology, Atmosphere and Ocean Research Institute, and National Institute for Environmental	Watanabe et al. (2011)
MIROC-ESM	Japan Agency for Marine-Earth Science and Technology, Atmosphere and Ocean Research Institute, and National Institute for Environmental	Watanabe et al. (2011)
MRI-CGCM3	Meteorological Research Institute, Japan	Yukimoto and Co-Authors (2012)
NorESM1-M	Norwegian Climate Centre, Norway	Bentsen et al. (2013)

Table 1: List of models used in this compilation

To keep the data volume within reasonable bounds, only the first ensemble member of each model was included here (ensemble member 1). While this selection limits to some degree the representation of the full internal variability within each model at regional scales (Deser et al. 2012), having 16 different models effectively compensates for this problem. While all individual model outcomes are provided, the reliance on single realizations from a single model should therefore be discouraged and consultation of the ensemble information is necessary to achieve reasonably robust results. Overall, the users of the CCKP need to be made aware of these issues related to internal climate variability.

The raw model information was derived from the Earth System Grid distribution of CMIP (<http://pcmdi9.llnl.gov/esgf-web-fe/>). For each model (see Table 1), a section of the *historical* simulations were required to form each model's own reference period. While generally the World Meteorological Organization prefers reference periods that span 30 years (e.g., 1971-2000, or 1981-2010), the IPCC-AR5 (Stocker et al. 2013) broadly utilized a **20-year interval of 1986-2005**. This period covers the final 20 years of the *historical* simulations that were driven with observed radiative forcings. A 20-year window also corresponds to the CCKP requested 20-year climatological windows for the future, namely 2020-2039, 2040-2059, 2060-2079, and 2080-2099. For each of these future time windows, simulations from all four RCPs were obtained and processed for the variables of (1) near surface monthly mean air temperature (tas), (2) near surface mean daily minimum temperature (tasmin), (3) near surface mean daily maximum temperature (tasmax), and (4) monthly precipitation sums (pr).

DATA PROCESSING STEPS AND THE EVALUATION PROTOCOL

The original CMIP5 model simulations had to be processed separately to establish a common dataset for which both absolute climatologies for the present and future 20-year intervals (see above) as well as their relative changes in comparison to their common reference period of 1986-2005 could be computed. While the base-data was obtained as monthly time series, the products were to represent 20-year climatologies. The shorter averaging interval of only 20-years rather than the traditional 30-year climatologies suggested by the World Meteorological Organization might introduce slightly larger noise resulting from the smaller sample size. But at the same time, the 20-year intervals become more useful when looking at the progressive changes throughout the 21st century with its continuously shifting climate. Each 20-year time windows can therefore be compared to the standard “present day” period of 1986-2005. The resulting anomalies also correspond well to results presented in the IPCC (Stocker et al. 2013).

The following steps describe how each of the selected models were processed:

1. **Re-gridding:** Initially, because all original model output is offered on their own native grids, the multi-model collection needed to be re-gridded to a common resolution. Data presented previously through the CCKP has been using a half-degree (0.5°x0.5°) grid. That grid spacing represents a significantly higher resolution than most of the global models in CMIP3 as well as CMIP5. In consultation with the World Bank CCKP team, and in order not to imply a false promise of high-resolution content in the GCM data, a new common 1°x1° global grid spacing was produced through bi-linear interpolation. This resolution is slightly coarser than CMIP3 data, yet it contains at least the same information detail as before, particularly since the underlying models sometimes improved their resolutions since CMIP3. All analyses and data products within the CCKP CMIP5 distribution exclusively utilize these re-gridded data.

2. Climatologies: For each model, and for each of the four selected variables, 20-year climatologies were formed. The ‘baseline’ interval (1986-2005) was derived from the *historical* simulations, while the future climatologies (2020-2039, 2040-2059, 2060-2079, 2080-2099) were computed for all four RCPs (rcp2.6, rcp4.5, rcp6.0, rcp8.5). These climatologies consist of 12 monthly average values and one annual mean value established over the respective time windows (sums for precipitation). To form the climatologies, all values were computed directly from the absolute temperature and precipitation data taken from the model simulations. Note, each model might exhibit slightly different absolute temperatures and precipitation. These offsets compared to observational data are generally small, yet in some regions they can be significant. In fact, because of these offsets in the depiction of climate in absolute values, the climatologies don’t lend themselves easily for model-to-model intercomparisons of change. Better suited are comparisons of relative changes (see below: anomalies).
3. Anomalies: For each model, each variable, and for each of the four future time windows, anomalies for each month as well as the annual value were computed and assessed relative to their corresponding *historical* reference period (1986-2005). In contrast to the climatologies, these values are well suited for model-to-model intercomparisons as they always refer to the change simulated by each model.
4. Ensemble information: The anomalies from each of the models in the collection, and for every 20-year climatological period in the future, ensemble values were calculated that describe how the collection of 16 CMIP5 models on average project the climatological changes using the median of the individual model values. Next to that central value of the ensemble, also ensemble high (90th-percentile) and low (10th-percentile) values for all the climatological anomalies were generated to help users recognize the range of likely outcomes driven by the different sources of uncertainty. Because each model has slightly different climate sensitivity and simulated different internal climate variability, the projections increasingly diverge into the future. Therefore, the ensemble spread increases with time. Note, each individual model’s anomalies can be compared with the provided ensemble description that encompasses the range between high (90th percentile) and low (10th percentile) levels of the underlying distribution.
5. Climatological ensemble based on observational basis: A second ensemble product is provided as a condensed climatological description in absolute values of the projected changes across the multi-model collection. This ensemble is the combination of the absolute values from a common observational baseline dataset and the superposed multi-model ensemble anomalies (note, only the ensemble quantities are used, not each model’s climatologies). The result is a description in absolute units of projected future climate as represented by the 90th-percentile, the median (the 50th-percentile), and the 10th-percentile series derived from the 16-models. The baseline was taken from the University of East Anglia, Climatic Research Unit (CRU) Time Series (TS) Version 3.21 dataset (Jones and Harris 2013), a globally gridded dataset with a nominal resolution of 0.5°x0.5°. This reference data was interpolated using a bi-linear scheme to the same 1°x1° grid as the CMIP5 data. The two products were then added.

The intent of this ensemble is to provide users a condensed perspective in absolute values of projected future climate with its most faithful representation of uncertainty. Because individual models might potentially exhibit substantial biases, this composite approach of an ensemble characterization is significantly more useful for depicting the future climate than a direct ensemble visualization generated on the raw climatologies of each of the individual climate model. Because of the biases, it is not recommended to plot the individual raw, absolute model

climatologies together with the condensed ensemble ranges. Equally, just plotting the individual climatologies and forming an “on-the-fly” ensemble is not meaningful because the majority of differences (spread) is based simply on biases in each of the individual climate models and not a faithful representation of the true physical uncertainty.

6. Quality Control: Because of the large data volumes, not every field individually could be visual inspected. Rather, NCAR implemented an automated final quality control algorithm on the publication-ready data to identify odd outliers in both absolute and anomaly fields. Suspicious values and potentially suspicious model simulations were flagged and ultimately 4 models were excluded from the results.

The data tables were provided for the following spatial aggregation categories: Basins, countries and regions. Figure 1 provides a global overview of this spatial sub-setting.

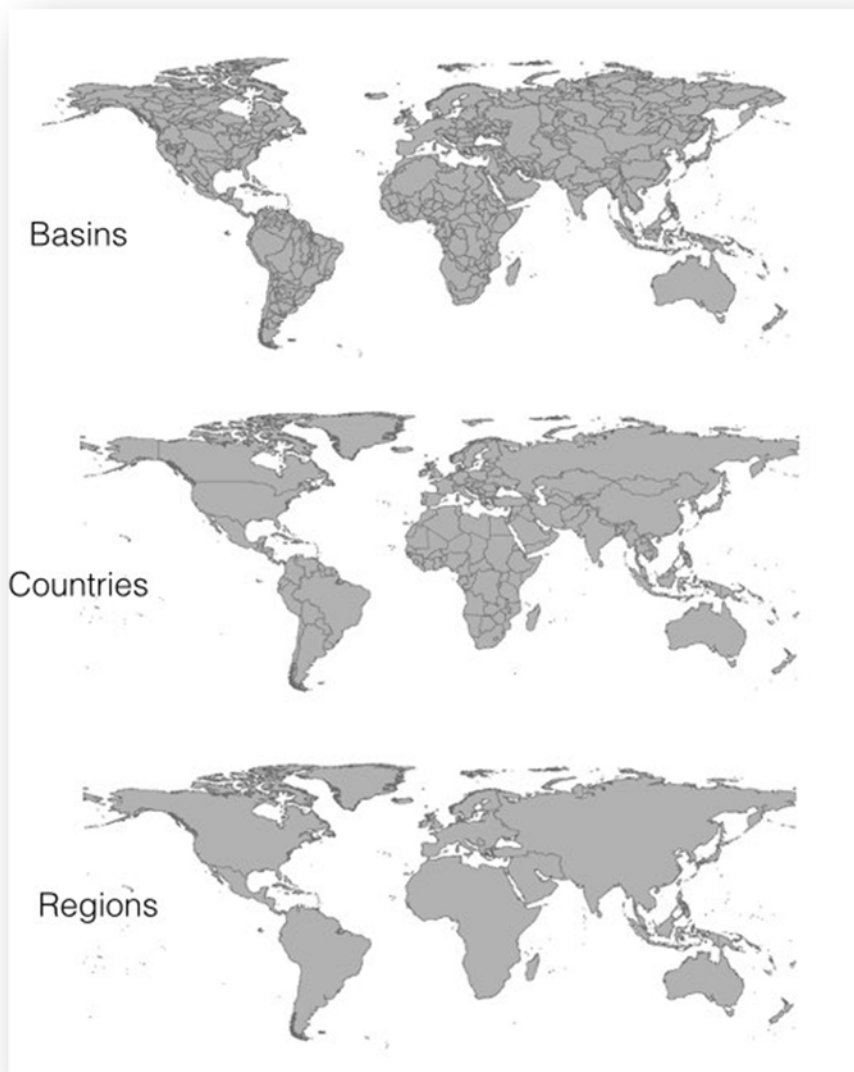


Figure 1: Map representation of the three regional aggregations

CMIP3 Dataset

CREDITS: Climate Systems Analysis Group, University of Cape Town.

LINK: www.csag.uct.ac.za

DESCRIPTION:

Future information is derived from 15 of the 23 available [global circulation models \(GCMs\)](#), the most comprehensive physically-based models of climate change available and used by the [Intergovernmental Panel on Climate Change \(IPCC\) 4th Assessment Report](#). The models are useful to illustrate the changing nature of large scale climate dynamics on continental to global scales and form the basis for understanding the human induced changes in climate. Because the resolution of these GCMs varies, they were re-gridded to a common 2° grid as in [this MAP](#).

Mean and change from the historical period to selected future time periods (see below) for the following variables

- Rainfall, and Temperature for all 15 models [View Models](#) <link to models list at the end of this document (in a new page)
- For 9 of the global circulation models, several statistics are available, including - Frost days, Heat wave duration, Maximum 5 day precipitation, with ppt > 90th percentile, ,, mean daily rainfall, total monthly rainfall, mean maxT/minT, number, hot days (90th %), cold days (10th %), cold nights (10% of tmin, warm nights (tmin90th %), frost days (Tmin < zero).

There are two scenarios that describe future economic growth and energy and they are important tools for understanding the long-term consequences of climate change. Emissions scenarios are often based on different storylines of economic and population growth, energy efficiency, and concern for environmental sustainability. Corresponding levels of emissions of greenhouse gases and other factors may be deduced from these storylines. Future projections are available for two of these storylines:

- The A2 storyline - is a case of rapid and successful economic development, in which regional average income per capita converge - current distinctions between "poor" and "rich" countries eventually dissolve.
- The B1 storyline - The central elements of the B1 future are a high level of environmental and social consciousness combined with a globally coherent approach to a more sustainable development. Heightened environmental consciousness might be brought about by clear evidence that impacts of natural resource use, such as deforestation, soil depletion, over-fishing, and global and regional pollution, pose a serious threat to the continuation of human life on Earth. In the B1 storyline, governments, businesses, the media, and the public pay increased attention to the environmental and social aspects of development. Technological change plays an important role. At the same time, however, the storyline does not include any climate policies, to reflect the SRES terms of reference. Nevertheless, such a possible future cannot be ruled out.

Future Time Periods

- 20 year averages and change from the historical time period for each model across the following time periods:
 - 2020-2039
 - 2040-2059
 - 2060-2079
 - 2080-2099

Climate Change and projections used in the table. To learn more click [here](#)

Access future climate data: navigate through map>climate tab>future tab

IMPACTS

AGRICULTURAL DATA

Rainfed/Irrigated Cultivated Land, Year 2000

CREDITS: Fischer, G., F. Nachtergaele, S. Prieler, H.T. van Velthuisen, L. Verelst, D. Wiberg, 2008

LINK: <http://app.databasin.org/app/pages/datasetPage.jsp?id=31abddefdcc247ca871f00a0de3ac2fd>

DESCRIPTION: Six geographic datasets were used for the compilation of an inventory of seven major land cover/land use categories at 5 degree resolution. The datasets used are:

1. GLC2000 land cover database at 30 arc-sec (<http://www-gvm.jrc.it/glc2000>), using regional and global legends;
2. an IFPRI global land cover categorization providing 17 land cover classes at 30 arc-sec. (IFPRI, 2002), based on a reinterpretation of the Global Land Cover Characteristics Database (GLCC ver. 2.0), EROS Data Centre (EDC, 2000);
3. FAOs Global Forest Resources Assessment 2000 (FAO, 2001) at 30 arc-sec. resolution;
4. digital Global Map of Irrigated Areas (GMIA) version 4.0 of (FAO/University of Frankfurt) at 5 by 5 latitude/longitude resolution, providing by grid-cell the percentage land area equipped with irrigation infrastructure;
5. IUCN-WCMC protected areas inventory at 30-arc-seconds (<http://www.unep-wcmc.org/wdpa/index.htm>), and
6. a spatial population density inventory (30-arc seconds) for year 2000 developed by FAO-SDRN, based on spatial data of LANDSCAN 2003, with calibration to UN 2000 population figures.

An iterative calculation procedure has been implemented to estimate land cover class weights, consistent with aggregate FAO land statistics and spatial land cover patterns obtained from (the above mentioned) remotely sensed data, allowing the quantification of major land use/land cover shares in individual 5 degree by 5 degree latitude/longitude grid cells. The estimated class weights define for each land cover class the presence of respectively cultivated land and forest. Starting values of class weights

used in the iterative procedure were obtained by cross-country regression of statistical data of cultivated and forest land against land cover class distributions obtained from GIS, aggregated to national level. The percentage of urban/built-up land in a grid-cell was estimated based on presence of respective land cover classes as well as regression equations relating built-up land with number of people and population density. Remaining areas were allocated to:

1. grassland and other vegetated areas (excluding cultivated land and forest);
2. barren or very sparsely vegetated areas, and
3. water bodies

according to indicated land cover classes. Barren or very sparsely vegetated areas (class (ii) above) were delineated from (i) using the respective land cover information in GLC 2000 and a minimum bio-productivity threshold.

The resulting seven land use land cover categories shares are:

1. Rain-fed cultivated land;
2. Irrigated cultivated land;
3. Forest;
4. Pastures and other vegetated land;
5. Barren and very sparsely vegetated land;
6. Water; and
7. Urban land and land required for housing and infrastructure.

Access Rainfed/Irrigated Cultivated Land, Year 2000: navigate through map>impacts tab>agriculture tab

LOW/HIGH INPUT, IRRIGATED/RAINFED CROPS

CREDITS: Fischer, G., F. Nachtergaele, S. Prieler, H.T. van Velthuisen, L. Verelst, D. Wiberg, 2007. Global Agro-ecological Zones Assessment for Agriculture (GAEZ 2007). IIASA, Laxenburg, Austria and FAO, Rome, Italy.

LINK: (link to document already in Portal)

DESCRIPTION: The datasets provided under this contract were calculated with the latest version of AEZ programs (termed GAEZ 2007) being published by IIASA and FAO. The files prepared for download on 19 May 2008 represent additions and a partial update of files provided to the World Bank's Climate Change Team in October 2007.

Access Low/High Input, Irrigated/Rainfed Crops: navigate through map>impacts tab>agriculture tab

GLOBAL IRRIGATED AREAS MAP

CREDITS: IWMI, [View Full Credits](#)

LINK: <http://www.iwmigiam.org/info/main/index.asp>

DESCRIPTION: This is the version 2.0 release (update; as of May 10, 2007) of the International Water Management Institute's (IWMI's) Global irrigated area map (GIAM) and associated products and data.

The GIAM products are produced using time-series data of: (a) AVHRR 10-km monthly from 1997-1999, (b) SPOT 1-km monthly for 1999, (c) GTOPO30 1-km elevation, (d) CRU 50-km grid monthly precipitation from 1961-2000, (e) AVHRR derived 1-km forest cover, and (f) AVHRR 10-km skin temperature. In addition JERS SAR data was used for the African and South American rainforests.

There are many unique features in the IWMI's GIAM product line. First, this is the very first satellite sensor based global irrigated area map. Second, the resolution of the map (10-km) is the best that is presently available for irrigated areas at global level. Third, the area calculations are done for each season. So the area irrigated @ the end of the last millennium for the entire world was: (a) 257 Mha during June-September, (b) 174 Mha during October-February, and (c) 41 Mha during March-May. Further, there is a flexibility to calculate areas every month. Fourth, this is NOT just a map. There are suite of products that consists of maps, images, class characteristics, area calculations, snap-shots and photos, animations, and accuracies. There are numerous advantages of such a product line. For example, disaggregated class images can be downloaded and a more refined map can be created with local expertise for one's area of interest. The irrigated areas are used to create a 20-year animations using AVHRR monthly time-series, so that one can spatially re-create the history of an irrigated area class. The class characteristics facilitate deriving crop calendar, sowing-peak-harvest dates of each class, and determine whether a class is single, double, or continuous crop. Fifth, the study develops and/or adopts a suite of innovative methods and techniques to map irrigated areas of the World at Global to local levels and at all resolutions or scale. The methods include spectral matching techniques (SMTs), image segmentation, decision tree algorithms and spatial modeling, data fusion, space-time spiral curves, brightness-greenness-wetness 2-dimensional feature space plots, NDVI time series plots, NDVI thresholds, principal component analysis, and unsupervised clustering algorithms. The wide array of ground truth data was also used. This included ground truth data of the Indus-Ganges river basins, Krishna river basin, IWMI's ground truth data of the World that included data for Middle East and Africa, the degree confluence project data of the world, and the 150-m Landsat geocover mosaic of the world.

Access Global Irrigated Areas Map: navigate through map>impacts tab>agriculture tab

GLOBAL MAP OF RAINFED CROPLAND AREAS

CREDITS: IWMI, [View Full Credits](#)

LINK: <http://www.iwmigiam.org/info/main/index.asp>

DESCRIPTION: The IWMI's Global Map of Rainfed Cropland Areas (GMRCA) is a by-product derived when working on IWMI's Global Map of Irrigated Areas (GMIA). The datasets approaches, and methods used to

produce GMRCA are, to a great extent, similar to producing GIAM. Thereby, we refer the reader to detailed documentation on GIAM made available in this web site.

The Global Rainfed Croplands were estimated at 1.132 billion hectares at the end of the last millennium, from the GMRCA products (Biradar et al., 2007). This is 2.78 times the TAAI or net irrigated areas (407 Mha) of the World. The GMRCA area provided here is for the June-October period only. Like, GMIA it is possible to estimate seasonal Global Rainfed Cropland areas using the products and methods developed in this study. However, double crop rainfed is considered negligible. The total cropland is estimated as 1.539 billion hectares of which 1.13 billion rainfed and 0.407 irrigated.

The importance of rainfed croplands cannot be over-emphasized. Rainfed croplands meet about 60 percent of the food and nutritional needs of the World's population, are backbone of the marginal or subsistence farmers, and are increasingly seen as better alternative to irrigated agriculture as a result of its environmental friendliness and sustainability over long time periods. Rainfed agriculture has an history of roughly 10,000 years compared to about 6000 year history of irrigated agriculture (see World resources 1992-1999, and Mackenzie and Mackenzie, 1995). Literature shows that the World's croplands increased from about 265 million hectares in year 1700 to about 1.4 billion hectares in 1990, of which rainfed cropland alone is about 1.2 billion hectares (Cramer and Soloman, 1993, Richards, 1990, Grubler, 1994, World Resources 1992-1999). Our estimate of rainfed croplands of the World, at the end of the millennium, is 1.13 billion hectares.

Most global digital maps (e.g., Loveland et al. 1999, Olson and Watts, 1982, Matthews, 1983) over estimate agricultural areas as a result of the pixel based area calculations (see Xiao, 1997, Cramer and Soloman, 1993). A pixel when classified as agriculture is automatically taken to have 100 % croplands in digital global maps. In reality only a certain percentage of a pixel is in cropland and that percentage can vary substantially. As a result the total agricultural lands estimated in various digital maps were 2.7 billion hectares by Olson and watts (1982) using a 50-km grid, 3.2 billion hectares by Matthews (1983) using 100-km grid, and 2.8 billion hectares by IGBP and USGS using 1-km grid (see Loveland et al. 1999). The FAO estimates based on Country statistics are closer to reality. The FAO statistics show cultivated areas at about 1.5 billion hectares (FAO, 2002). Grubler (1994) estimated that an increase of 1 billion arable lands would be needed for additional 5 billion world population in the 21st century.

The theoretical potential for cropland areas in the present climatic conditions and based on soil, climate, and topography are estimated at 3.29 billion hectares (Xiao et al. 1997) to 4.15 billion hectares (Cramer and Soloman, 1993). However, it must be noted that the productivity of a large proportion of these lands is limited due to poor soil fertility, soil depth, access to water, and disease (e.g., Tse-tse flies and the black fleas). Any increase will have to come from land conversions from forests and rangelands which will be environmentally costly (Richards, 1990) or from protected areas which is unacceptable.

In reality, cropland areas are shrinking in recent times as a result of soil degradation, urbanization, and desertification and global warming. Between the early 1960s and the late 1990s, world cropland grew by only 11 percent, while world population almost doubled. As a result, cropland per person fell by 40 percent, from 0.43 ha to only 0.26 ha and reduced from 0.23 to 0.11 hectares (FAO, 2002). In future, 80 percent of increased crop production in developing countries will have to come from intensification: higher yields, increased multiple cropping and shorter fallow periods.

Thereby, tracking changes in spatial distribution and changing patterns of rainfed croplands is essential for understanding and planning food and nutritional demands of expanding populations of the World.

In this context, the IWMI's GMRCA product-line provides a benchmark measure of Rainfed Cropland Areas of the World at the end of the last millennium. The sub-pixel area (SPAs) of GMRCA provides realistic estimates of the actual area cultivated unlike the full pixel areas (FPAs) of almost all other studies. The GMRCA product-lines have maps, images, area characteristics and calculations, snap-shots, and animations. In addition the satellite sensor data mega-files and the ground-truth data used to produce the GMRCA are made available.

There are two product-lines within GMRCA. These are:

1. Aggregated 9-class GMRCA map of the World; and
2. Dis-aggregated 67-class GMRCA map of the World.

The aggregated classes provide broad categories of rainfed cropland classes. Often, most users would just need such broad classes. The disaggregated classes provide a detailed picture and are often invaluable at regional, National, and local levels. For certain users, even at global level so that they can derive specific classes of interest to them. The class labeling in disaggregated classes are only indicative and can be improved.

Access Global Map of Rainfed Cropland Areas: navigate through map>impacts tab>agriculture tab

GLOBAL MAP OF IRRIGATION AREAS

CREDITS: Stefan Siebert, Petra Döll, Sebastian Feick, Jippe Hoogeveen and Karen Frenken (2007) *Global Map of Irrigation Areas version 4.0.1*. Johann Wolfgang Goethe University, Frankfurt am Main, Germany / Food and Agriculture Organization of the United Nations, Rome, Italy

LINK: <http://www.fao.org/nr/water/aquastat/irrigationmap/index10.stm>

DESCRIPTION: The latest version of the "Global Map of Irrigation Areas" is version 4.0.1. The map shows the amount of area equipped for irrigation around the turn of the 20th century in percentage of the total area on a raster with a resolution of 5 minutes. The area actually irrigated was smaller, but is unknown for most countries. A special note has to be made for Australia and India where the map shows the total area actually irrigated. This is due to the fact that statistics collected in Australia and India refer to actually irrigated area as opposed to statistics with area equipped for irrigation which are collected in most other countries. An explanation of the different terminology to indicate areas under irrigation is given in this [glossary](#).

The map is generated as a grid and distributed with the following characteristics:

Projection:	Geographic
Number of columns:	4320
Number of rows:	2160
North Bounding Coordinate:	90 degrees

East Bounding Coordinate: 180 degrees
South Bounding Coordinate: -90 degrees
West Bounding Coordinate: -180 degrees
Cellsize: 5 minutes, 0.083333 decimal degrees
NODATA values: Cells without irrigation are characterised by NODATA (-9), it does not mean that there was no data for these cells

For the GIS-users the map is distributed in two different formats: as zipped ASCII-grid that can be easily imported in most GIS-software that support rasters or grids; and, to accommodate people who use GIS-software that doesn't support rasters or grids, as a zipped ESRI shape file. It should be noted, however, that the values in the ASCII-grid have a precision of 6 decimals while the values in the shape-file have a precision of 2 decimals. For model calculations it is therefore recommended to use the grid-version. As a service to those people who would need to know the absolute area equipped for irrigation, another ASCII-grid is available in which the area equipped for irrigation is expressed in hectares per cell. Non-GIS-users can download the map as PDF-file in two different resolutions.

Access Global Map of Irrigation Areas: navigate through map>impacts tab>agriculture tab

HARVESTED AREA AND YIELDS (M3- CROPS DATA)

CREDITS: Monfreda et al. (2008), "Farming the planet: 2. Geographic distribution of crop areas, yields, physiological types, and net primary production in the year 2000", Global Biogeochemical Cycles, Vol.22, GB1022, doi:10.1029/2007GB002947

LINK: <http://www.geog.mcgill.ca/landuse/pub/Data/Agland2000/>

DESCRIPTION: Described in the publication, Monfreda et al. (2008), "Farming the planet: 2. Geographic distribution of crop areas, yields, physiological types, and net primary production in the year 2000", Global Biogeochemical Cycles, Vol.22, GB1022, doi:10.1029/2007GB002947. The data is provided in NetCDF and ArcGIS ASCII format at 5 minute resolution in latitude by longitude. The NetCDF files have 4 levels (ArcGIS files only have the 1st two levels; contact authors if you want the other two levels), as follows: Level 1 = Harvested Area (unit = proportion of grid cell area). Note that values can be greater than 1.0 because of multiple cropping. Level 2 = Yield (unit = tons per ha). Levels 3 and 4 = Administrative levels from which the source data in levels 1 and 2 come from respectively. In levels 3 and 4, a value of 1 = county; .75 = state; .5 = interpolated from within 2 degrees lat/long; .25 = country; 0 = missing.

Access Harvested Area and Yields (M3- Crops Data): navigate through map>impacts tab>agriculture tab

NATURAL HAZARDS

UNISDR GLOBAL ASSESSMENT REPORT (2015) RISK PLATFORM

DATASETS: TROPICAL CYCLONE, STORM SURGE, EARTHQUAKE, VOLCANIC ERUPTION, TSUNAMI, FLOOD

CREDITS: The Global Assessment Report 2015 is based on a joint effort by leading scientific institutions, governments, UN agencies and development banks, the private sector and non-governmental organisations. The CAPRA software used for visualization was developed by UNISDR in collaboration with the World Bank, Cimne, ERN and Ingeniar, with the generous financial support of the European Commission.

Link: <http://risk.preventionweb.net/capreviewer/main.jsp?countrycode=g15>

DESCRIPTION: in the UNISDR-led assessment, probabilistic hazard models have been developed for earthquake, tropical cyclone wind and storm surge, tsunami and river flooding worldwide, for volcanic ash in the Asia-pacific region and for drought in parts of Africa. The probabilistic hazard models were later used to inform the global risk model for each hazard type. The datasets and methods used to calculate probabilistic hazard is different for each hazard type. The return periods selected to be represented in the CCKP is different for each hazard. Global cyclone hazard data measured as wind speed that is expected to be exceeded at least once in a 100 year mean return period. Global storm surge hazard data measured as inundation height that is expected to be exceeded at least once in a 10 year mean return period. Global earthquake hazard data measured as ground motion intensity (pga) that is expected to be exceeded at least once in a 475 year mean return period. Global tsunami hazard data which is expected to occur at least once in 500 year mean return period. Global flood hazard data measured as inundation height that is expected to be exceeded at least once in 100 year mean return period.

More information and metadata/credits specific to each hazard type can be found [here](#).

Access Natural Hazards: navigate through map>impacts tab>natural hazards tab

GLOBAL RISK DATA PLATFORM

DATASETS: Wildfire, Drought, Earthquake-induced Landslides, Rainfall-induced Landslides

CREDITS: GIS processing UNEP/UNISDR

LINK: <http://preview.grid.unep.ch/index.php?preview=data&lang=eng>

DESCRIPTION: The Global Risk Data Platform is a multiple agencies effort to share spatial data information on global risk from natural hazards. Users can visualise, download or extract data on past hazardous events, human & economical hazard exposure and risk from natural hazards. It covers tropical cyclones and related storm surges, drought, earthquakes, biomass fires, floods, landslides,

tsunamis and volcanic eruptions. The collection of data is made via a wide range of partners (see About for data sources). This was developed as a support to the Global Assessment Report on Disaster Risk Reduction (GAR) and replace the previous PREVIEW platform already available since 2000. Many improvements were made on the data and on the application.

More information and metadata/credits specific to each hazard type can be found [here](#).

Access Natural Hazards: navigate through map>impacts tab>natural hazards tab

PACIFIC ISLANDS HAZARDS

DATASETS: Earthquake, Tropical Cyclone (for a selection of Pacific Islands)

CREDITS: PCRAFI - PCRAFI is a joint initiative of SOPAC/SPC, World Bank, and the Asian Development Bank with the financial support of the Government of Japan and the Global Facility for Disaster Reduction and Recovery (GFDRR), and technical support from AIR Worldwide, NZ GNS Science, Geoscience Australia, Pacific Disaster Center (PDC), OpenGeo and GFDRR Labs

LINK: <http://pcrafi.sopac.org/>

DESCRIPTION: The Pacific Catastrophe Risk Assessment and Financing Initiative (PCRAFI) aims to provide the Pacific Island Countries (PICs) with disaster risk modeling and assessment tools. PCRAFI produced detailed probabilistic hazard models for all 15 countries, such as Tropical Cyclones with Winds, Storm Surge, Rain Earthquake with Ground-shaking, and Tsunami. The information displayed on the CCKP are earthquake hazard data measured as ground motion intensity (PGA) that is expected to be exceeded at least once in 100 year mean return period, and tropical cyclone hazard data measured as wind intensity that is expected to be exceeded at least once in 100 year mean return period.

More information and metadata/credits specific to each hazard type can be found [here](#).

Access Pacific Island Hazards: navigate through map>impacts tab>natural hazards tab

EM-DAT

INFORMATION: Top disasters (number killed), Number of affected, Average annual disaster occurrence by type.

CREDITS: EM-DAT: The OFDA/CRED International Disaster Database – www.emdat.be – Université Catholique de Louvain – Brussels – Belgium.

LINK: <http://www.emdat.be/>

DESCRIPTION: EM-DAT contains essential core data on the occurrence and effects of over 18,000 mass disasters in the world from 1900 to present. The database is compiled from various sources, including

UN agencies, non-governmental organisations, insurance companies, research institutes and press agencies.

Access EM-DAT: navigate through map>impacts tab>natural hazards tab

WATER DATA

WATER INDICATOR

DATASETS: Flood Indicator, Drought Indicator, Mean Annual Runoff, Annual Base Flow, Storage, Mean Annual Irrigation Deficit

CREDITS: Strzepek, K., McCluskey, A., Boehlert, B., Jacobsen, M., & Fant IV, C. (2011). *Climate Variability and Change: A Basin Scale Indicator Approach to Understanding the Risk to Water Resources Development and Management*. The World Bank.

LINK: View Paper: Climate Variability and Change: A Basin Scale Indicator Approach to Understanding the Risk to Water Resources Development and Management.

DESCRIPTION: This study evaluates the effects of climate change on six hydrological indicators across 8,413 basins in World Bank client countries. These indicators—mean annual runoff (MAR), basin yield, annual high flow, annual low flow, groundwater (baseflow), and reference crop water deficit—were chosen based on their relevance to the wide range of water resource development projects planned for the future. To generate a robust, high-resolution understanding of possible risk, this analysis examines relative changes in all variables from the historical baseline (1961 to 1999) to the 2030s and 2050s for the full range of 56 General Circulation Model (GCM) Special Report on Emissions Scenario (SRES) combinations evaluated in the Intergovernmental Panel on Climate Change (IPCC) Fourth Assessment Report (AR4).

Access Water Indicators: navigate through map>impacts tab>water tab

AQUASTAT

CREDITS: FAO

LINK: <http://www.fao.org/nr/water/aquastat/main/index.stm>

DESCRIPTION: AQUASTAT is FAO's global information system on water and agriculture, developed by the Land and Water Division. The main mandate of the programme is to collect, analyze and disseminate information on water resources, water uses, and agricultural water management with an emphasis on countries in Africa, Asia, Latin America and the Caribbean. This allows interested users to find comprehensive and regularly updated information at global, regional, and national levels.

In AQUASTAT, three types of water withdrawal are distinguished: agricultural, municipal (including domestic), and self-abstracted industrial water withdrawal. A fourth type of anthropogenic water use is

the water that evaporates from artificial lakes or reservoirs associated with dams. Information on evaporation from artificial lakes will be available in the AQUASTAT database in the near future.

At global level, the withdrawal ratios are 70 percent agricultural, 11 percent municipal and 19 percent industrial. These numbers, however, are biased strongly by the few countries which have very high water withdrawals. Averaging the ratios of each individual country, we find that "for any given country" these ratios are 59, 23 and 18 percent respectively.

For Africa, Asia, Latin America and the Caribbean, AQUASTAT obtains water withdrawal values from ministries or other governmental agencies at a country level, although some data gaps are filled from UN Data. For Europe and for Northern America, Japan, Australia and New Zealand, Eurostat and OECD are valuable sources of information, and also used to fill data gaps.

Access Aquastat: navigate through map>impacts tab>water tab

VULNERABILITIES

GRIDDED POPULATION OF THE WORLD, VERSION 3 (GPWV3) DATA COLLECTION

CREDITS: CIESIN, Centro Internacional de Agricultura Tropical (CIAT)

LINK: <http://sedac.ciesin.columbia.edu/gpw/metadata1.jsp>

DESCRIPTION: Gridded Population of the World, Version 3 (GPWv3) consists of estimates of human population for the years 1990, 1995, and 2000 by 2.5 arc-minute grid cells and associated datasets dated circa 2000. The data products include population count grids (raw counts), population density grids (per square km), land area grids (actual area net of ice and water), mean administrative unit area grids, centroids, a national identifier grid, national boundaries, and coastlines. These products vary in GIS-compatible data formats and geographic extents (global, continent [Antarctica not included], and country levels). A proportional allocation gridding algorithm, utilizing more than 300,000 national and sub-national administrative units, is used to assign population values to grid cells. GPWv3 is produced by the Columbia University Center for International Earth Science Information Network (CIESIN) in collaboration with Centro Internacional de Agricultura Tropical (CIAT).

Access GPWv3: navigate through map>vulnerabilities tab>population icon

POVERTY MAPPING PROJECT: GLOBAL SUBNATIONAL PREVALENCE OF CHILD MALNUTRITION

CREDITS: CIESIN

LINK:

http://sedac.ciesin.org/povmap/downloads/ds_global/metadata/PovertyMappingProjectGlobalSubnationalPrevalenceofChildMalnutrition.htm

DESCRIPTION: The Global Subnational Prevalence of Child Malnutrition dataset consists of estimates of the percentage of children with weight-for-age z-scores that are more than two standard deviations below the median of the NCHS/CDC/WHO International Reference Population. Data are reported for the most recent year with subnational information available at the time of development. The data products include a shapefile (vector data) of percentage rates, grids (raster data) of rates (per thousand in order to preserve precision in integer format), the number of children under five (the rate denominator), and the number of underweight children under five (the rate numerator), and a tabular dataset of the same and associated data. This dataset is produced by the Columbia University Center for International Earth Science Information Network (CIESIN).

Access GPWv3: navigate through map>vulnerabilities tab>nutrition icon

OTHER

WORLD BANK PROJECTS

CREDITS: The World Bank Group

LINK: <http://maps.worldbank.org/>

DESCRIPTION: Mapping for Results (maps.worldbank.org) has provided the location data of all active World Bank-financed projects under the following product lines: IBRD/IDA, Global Environment Project, Special Financing, Montreal Protocol, GEF Medium Sized Programs, Guarantees, Debt Reduction Facility, Carbon Offsets, and large Recipient-Executed Activities. Locations of mapped projects are as of June 30, 2011.

Access World Bank Projects: navigate through map> >World Bank icon

WATERBASE GLOBAL RIVER BASINS

CREDITS: United Nations University

LINK: http://www.waterbase.org/download_data.html

DESCRIPTION: Shapefiles for river basins across the world are available from WaterBase, divided into continents: Africa, Asia, Australasia, Europe, North America, South America. The WaterBase project is an ongoing project of the United Nations University. Its aim is to advance the practice of Integrated Water Resources Management (IWRM) in developing countries.

Access Global River Basins: navigate through map to river basin level

LOW CARBON GROWTH STUDIES

CREDITS: ESMAP

LINK: <http://www.esmap.org/esmap/lcgs>

DESCRIPTION: Emerging economies have a different set of energy issues from low-income countries, and several governments are already taking steps to study alternative scenarios for a shift towards a low carbon growth trajectory. With the help of ESMAP's Low Carbon Growth Studies Pilot Project (2007–09), the governments of six middle-income-countries—Brazil, China, India, Indonesia, Mexico, and South Africa—assessed their development goals and priorities for GHG mitigation. The studies considered the additional costs and benefits of lower carbon growth and how to finance such measures.

Access GPWv3: navigate through map>